Neural, Parallel, and Scientific Computations 28 (2020) No.4, 223-245

THE ROLE OF RISK AVERSION IN STOCHASTIC DIFFERENTIAL REINSURANCE GAMES

NEGASH G. MEDHIN AND CHUAN XU

Department of Mathematics, North Carolina State University, Raleigh, NC 27629-8205, USA.
SAS Institute, Cary, NC 27513-2414, USA.

ABSTRACT. In this paper, the role of risk aversion in stochastic reinsurance games is investigated. The state of diffusion processes in reinsurance games can be fully characterized by probability density functions (PDFs). Therefore, we derive the associated PDFs by the Fokker-Planck equation (FPE). General PDFs, adapted to high dimensions and with covariance terms, are given. The Chang-Cooper scheme is extended to the high dimensions to perform numerical analysis for our problem. The scheme is validated by an example first to show the accuracy. Then, a procedure based on the previous scheme is developed to study the relationship between the risk aversion coefficient and the expected utility of terminal wealth for reinsurance games numerically. With the procedure, we can show the trend between the two. In our case, a larger risk aversion results in higher terminal wealth. However, the benefit of raising risk aversion decays significantly after certain thresholds. For comparison, the Monte-Carlo method is also applied, and the result reveals the same pattern as before.

AMS (MOS) Subject Classification. 91A15, 37N30.

1. Introduction

Risk aversion consideration plays an essential role in many fields, such as actuarial science, investment, finance, economics. [8] studied the risk aversion in optimal investment decision with an expected utility function. The relationship between the risk aversion and incentive effects was studied in [11] with empirical data. [23] showed that the elasticity of the intertemporal substitution between the consumption and stock-market participation is consistent with plausible values of the risk aversion coefficient when using a specific preference. Due to the importance of the risk aversion in real-world applications, multiple ways are developed to measure and estimate it. [13] derived risk aversion functions implied by option prices and realized returns on the S&P500 index and estimate the coefficient with a derived function. A dynamic way to estimate the investor risk aversion from option-implied and realized volatilities

Received November 1, 2020 1061-5369 $15.00 ©Dynamic Publishers, Inc.
www.dynamicpublishers.org; www.dynamicpublishers.com;
https://doi.org/10.46719/npsc20202841.

was developed in [4]. [22] proposed using the Taylor series expansion for inferring risk aversion coefficients to overcome some challenges in previous estimation methods. [3] considered two types of utility functions: the exponential and quadratic utility function. Analytic expressions for the risk aversion coefficient as a function of the VaR level were given in [3].

The non-cooperative game is not new. Many studies have been done with this type of structure. [12] proposed an advertising game model for the manufacturer-retailer supply chain, which covers two cooperative models and one non-cooperative model. A similar problem was studied in [19]. In the latter paper, a specific marketing strategy, vertical cooperative advertising along with price decisions, was considered. Three non-cooperative games, including the Nash, Stackelberg-manufacturer, Stackelberg-retailer, and one cooperative game were covered in the study. In these papers, the constraints of control problems are pretty simple and straightforward. The equilibriums are not difficult to derive. They focus more on the discussion about what the results could bring to us. In addition to the two papers, non-cooperative game models are widely applied in many fields. Nevertheless, what kind of role the risk aversion factor plays in such games was rarely studied even though the risk aversion is vital in real-world decision problems.

In [16], we have discussed the stochastic reinsurance differential game, which is governed by jump-diffusion processes. Now, a little further, we would like to study the role risk aversion plays in reinsurance games. The state of stochastic processes can be fully characterized by its statistical distribution, which is represented by the probability density functions (PDFs). The evolution of the PDFs associated with the diffusion processes in reinsurance games can be derived from the Fokker-Planck equation (FPE). With the PDFs, the problem is transformed from stochastic to deterministic. Then, with proper approximations to the FPEs, which are parabolic partial differential equations, the impacts of different risk aversion levels on the expected utility of terminal wealth can be explored.

The Fokker-Planck equation was introduced by Adriaan Fokker and Max Planck to describe the time evolution of the PDF of the position and velocity of a particle, which is one of the classical widely used equations of statistical physics. FPE is one of the most fundamental equations in physics and plays an essential role in every area of science. For example, [20] approximated the chemical master equation with a continuous FPE using sparser computational grids. Then, the performance of the numerical solution is compared with the standard Monte Carlo simulation algorithm. The result shows that the FPE method is well suited for low-dimensional, high-accuracy desirable problems. [10] studied a bilinear control problem subject to FPEs where controls depend on time and space. The existence of optimal controls was proved, and the first-order necessary optimality conditions were derived.

Despite the importance of the FPE, however, most FPEs do not have an exact analytic solution, and therefore, approximation and numerical approaches are necessary. The commonly used methods are the adomian decomposition method (ADM), variational iteration method (VIM), homotopy perturbation method (HPM), method of lines, finite difference method, Fourier method, operator method, path integral method, and finite element method.

Assuming that $A(x,t), B(x,t)$ and $C(x,t)$ in the general FPE are all positive functions, [6] proposed a finite difference scheme for initial value problems of one-dimension FPEs. This scheme provides non-negative, particle conserving numerical solutions, which are exact representations of the analytic solution upon equilibrium. [6] proved that the positiveness of the solution, conservation of particles, and accuracy of the equilibrium solution could be guaranteed with such choice of δ_j.

[15] proposed several new numerical methods for solving a general class of linear and nonlinear one-dimension time-dependent FPE. Built on [6], [15] remedied certain shortcomings of the Chang-Cooper scheme. [5] shows that for a particular linear FP operator, the explicit Chang-Cooper scheme is positive and entropy satisfying under a Courant-Friedrichs-Levy (CFL) criterion when the initial conditions are positive. Following [6], [18] developed an accurate second-order method that does not impose any restrictions on the mesh size and is capable of capturing the asymptotic steady states with arbitrary accuracy.

Combining the Chang-Cooper scheme and receding horizon model predictive control (RHMPC) scheme, [2] studied an optimal control problem. In the paper, optimization problems are formulated as a sequence of open-loop optimality systems in a receding-horizon control strategy. Then, the system is discretized by the Chang-Cooper scheme to guarantee the positivity of the forward solution. The result is validated with a stochastic Lotka-Volterra model and a noised limit cycle model. [17] gave more details on the problem and showed that Chang-Cooper scheme combined with the backward first-order and second-order finite differencing in time provides stable and accurate solutions.

In this study, the main question we are interested in is: what does the role of risk aversion play in the stochastic differential reinsurance game? Based on our review, no studies have been done to reveal the exact relationship between the two. The traditional method on reinsurance games, by the Hamilton-Jacobi-Bellman (HJB) equation, has been explored in [16]. In this study, we would like to try another way to tackle our principal problem. One classic stochastic control design is taking the expectation of some utility functions depending on the path of the stochastic process as the objective function. However, as pointed out in [14], this could be troublesome sometimes due to, e.g., computational demand. The PDF can also describe the full state of the stochastic process, which makes FPE is an excellent alternative to the classic method contingent upon the users' resources. For example, taking expectation is no longer needed when the Kullbak-Leibler or square distance between the target and current PDF is applied as the objective function.

Moreover, by a suitable numerical approximation method of the FPE, problems can get solved efficiently by a discretization scheme based on the approximation method after target PDFs are chosen by users, as shown in [1]. Consequently, our target is to develop a FPE-based procedure working for the general stochastic control problem. The procedure should overcome the limitations, e.g., restraints on the dimensionality or covariance matrix, and assumptions based on the physical properties.

The outline of this research is as follows. In section 2, the FPE for diffusion processes in the stochastic reinsurance game is derived to transform the problem into a control problem governed by the PDF instead of the stochastic processes. In section 3, the details of the Chang-Cooper scheme for the high-dimensional FPE with covariance terms are discussed at the beginning. Then, we validate the accuracy of our scheme with a numerical example; at last, the relationship between the risk aversion coefficient b and expected utility of terminal wealth $E[J(X_T)]$ is studied to show the impacts of risk aversion in reinsurance games. Section 4 gives a summary of our results and concluding remarks.

2. **The Fokker-Planck Equation of the Game**

Based on [16], a formulation for the duopoly stochastic reinsurance differential game is:

$$
\begin{cases}
\max\limits_{\Pi_1} \quad E[J(X_T)] \\
\max\limits_{\Pi_2} \quad E[J(Y_T)] \\
\text{s.t.} \\
X_t = X_0 + \displaystyle\int_0^t [r(X_s - (u_s^1)^2) + (\mu_1 - r)A_s^1 + (c_1 - \delta(q_1))(p_1 u_s^1 + \eta)H \\
\qquad - (c_1 - \delta(q_1))(p_1 u_s^1 + p_2 u_s^2 + 2\eta)M_s]ds + \displaystyle\int_0^t A_s^1 \sigma_1 dW_s^1 \\
\qquad + \displaystyle\int_0^t (c_1 - \delta(q_1))\sigma_m dW_s^3 - q_1 \sum_{i=1}^{N_t^1} Z_i^1, \\
Y_t = \displaystyle\int_0^t [r(Y_s - (u_s^2)^2) + (\mu_2 - r)A_s^2 - (c_2 - \delta(q_2))(p_1 u_s^1 + \eta)H \\
\qquad + (c_2 - \delta(q_2))(p_1 u_s^1 + p_2 u_s^2 + 2\eta)M_s]ds + \displaystyle\int_0^t A_s^2 \sigma_2 dW_s^2 \\
\qquad - \displaystyle\int_0^t (c_2 - \delta(q_2))\sigma_m dW_s^3 - q_2 \sum_{i=1}^{N_t^2} Z_i^2, \\
M_t = M_0 + \int_0^t [(p_1 u_s^1 + \eta)H - (p_1 u_s^1 + p_2 u_s^2 + 2\eta)M_s]ds + \int_0^t \sigma_m dW_s^3, \\
M_0 \in [0, H].
\end{cases}
\tag{2.1}
$$

where X_t, Y_t are the wealth of the insurance company A and B at time t; r is the risk-free rate; u_t^i, A_t^i are the controls over the advertising and investment at time t; p_i is the advertising effectiveness coefficient; η is the market share decay constant; c_i is the insurance premium rate; H is the maximal market potential; q_i is the retention rate; M_t is the market share of the insurance company A at time t; $\sigma_1, \sigma_2, \sigma_m$ are the constant diffusion coefficients; W_t^1, W_t^2, W_t^3 are standard Wiener processes; S_t^i is a compound Poisson process; $J(\cdot)$ is an utility function depending on the terminal wealth. In addition, we have $E[W_t^1 W_t^3] = \rho_1 t$, $E[W_t^2 W_t^3] = \rho_2 t$ where ρ_1, ρ_2 are correlation coefficients. More details about the formulation can be found in the paper mentioned above.

First, let us introduce the following theorem:

Theorem 2.1. *Suppose we have two diffusion processes:*

$$\begin{cases} X_t := X_0 + \int_0^t b(s, X_s, M_s)ds + \int_0^t \sigma(s, X_s, M_S)dB_s - \sum_{i=1}^{N_t} Y_i, \\ M_t := M_0 + \int_0^t b_1(s, X_s, M_s)ds + \int_0^t \sigma_1(s, X_s, M_s)dB_s^1, \end{cases} \tag{2.2}$$

where $E[\int_0^t \sigma(s, X_s, M_s)ds] < \infty$ and $E[\int_0^t \sigma_1(s, X_s, M_s)ds] < \infty$, B_t and B_t^1 are two independent standard Wiener processes, $Z_t = \sum_{i=1}^{N_t} Y_i$ is a compound Poisson process where Y_i is I.I.D., N_t is a Poisson process with the intensity λ. Then, the Fokker-Planck equation is

$$\begin{aligned} \frac{\partial P(t,x,m)}{\partial t} = &- \left[\frac{\partial[P(t,x,m)b(t,x,m)]}{\partial x} - \lambda E[Y]\frac{\partial P(t,x,m)}{\partial x}\right] - \frac{\partial[P(t,x,m)b_1(t,x,m)]}{\partial m} \\ &+ \frac{1}{2}\left[\frac{\partial^2[P(t,x,m)\sigma^2(t,x,m)]}{\partial x^2} + \lambda E[Y^2]\frac{\partial^2 P(t,x,m)}{\partial x^2}\right] \\ &+ \frac{1}{2}\frac{\partial^2[P(t,x,m)\sigma_1^2(t,x,m)]}{\partial m^2}, \end{aligned} \tag{2.3}$$

where $P(t,x,m)$ is the joint probability density for (X_t, M_t).

Proof. First, since the compound Poisson process is a Lévy process, then definitely X_t is a Lévy process which has the Markov property. Then for any continuous state Markov processes, we have the following Chapman-Kolmogorov equation:

$$\begin{aligned} &P(X_{t_3}, M_{t_3}, t_3 | X_{t_1}, M_{t_1}, t_1) \\ &= \int_{(X_{t_2}, M_{t_2})\in\Omega} P(X_{t_3}, M_{t_3}, t_3 | X_{t_2}, M_{t_2}, t_2) P(X_{t_2}, M_{t_2}, t_2 | X_{t_1}, M_{t_1}, t_1) d\Omega, \end{aligned} \tag{2.4}$$

where $P(\cdot|\cdot)$ is the transition probability of (X_t, M_t).

Consider a differentiable function $f(t, X_t, M_t) = f(x, m, t)$ with $f(t, X_t, M_t) = 0$ for $t \notin (0, T)$. With Proposition 8.13 of [7], we have:

$$\begin{aligned} df(t, X_t, M_t) = &\left(\frac{\partial f}{\partial t} + \frac{\partial f}{\partial x}b + \frac{\partial f}{\partial m}b_1 + \frac{1}{2}\frac{\partial^2 f}{\partial x^2}\sigma^2 + \frac{1}{2}\frac{\partial^2 f}{\partial m^2}\sigma_1^2\right) dt \\ &+ \frac{\partial f}{\partial x}\sigma dB_t + \frac{\partial f}{\partial m}\sigma_1 dB_t^1 + \left[f(t, X_{t-} - Y, M_t) - f(t, X_{t-}, M_t)\right], \end{aligned} \tag{2.5}$$

for simplicity, we write $b(s, X_s, M_s), \sigma(s, X_s, M_S), b_1(s, X_s, M_s), \sigma_1(s, M_S)$ as b, b_1, σ, σ_1.

Hence, from (2.5), we have:

(2.6)
$$f(T, X_T, M_T) - f(0, X_0, M_0) = \int_0^T \left(\frac{\partial f}{\partial t} + \frac{\partial f}{\partial x}b + \frac{\partial f}{\partial m}b_1 + \frac{1}{2}\frac{\partial^2 f}{\partial x^2}\sigma^2 + \frac{1}{2}\frac{\partial^2 f}{\partial m^2}\sigma_1^2\right) dt$$
$$+ \int_0^T \frac{\partial f}{\partial x}\sigma dB_t + \int_0^T \frac{\partial f}{\partial m}\sigma_1 dB_t^1$$
$$+ \int_0^T \int_{\mathbb{R}} f(t, X_{t-} - y, M_t) - f(t, X_{t-}, M_t) J_X(dydt),$$

where J_X is the Poisson random measure defined as in Section 2.6 of [7] and with the intensity $\mu(dtdy) = \lambda dt F(dy)$.

Take expectation on both sides of (2.6), then:

(2.7)
$$E[f(T, X_T, M_T)] - f(0, X_0, M_0) = E[\int_0^T \left(\frac{\partial f}{\partial t} + \frac{\partial f}{\partial x}b + \frac{\partial f}{\partial m}b_1 + \frac{1}{2}\frac{\partial^2 f}{\partial x^2}\sigma^2 + \frac{1}{2}\frac{\partial^2 f}{\partial m^2}\sigma_1^2\right) dt]$$
$$+ E[\int_0^T \int_{\mathbb{R}} f(t, X_{t-} - y, M_t) - f(t, X_{t-}, M_t) J_X(dtdy)]$$
$$= E[\int_0^T \left(\frac{\partial f}{\partial t} + \frac{\partial f}{\partial x}b + \frac{\partial f}{\partial m}b_1 + \frac{1}{2}\frac{\partial^2 f}{\partial x^2}\sigma^2 + \frac{1}{2}\frac{\partial^2 f}{\partial m^2}\sigma_1^2\right) dt]$$
$$+ E[\int_0^T \lambda \int_{\mathbb{R}} f(t, X_{t-} - y, M_t) - f(t, X_{t-}, M_t) F(dy)dt].$$

Considering the second term on the right first, since $f(\cdot)$ is a differentiable function, then we take Taylor's expansion:

(2.8)
$$E[\int_0^T \lambda \int_{\mathbb{R}} f(t, X_{t-} - y, M_t) - f(t, X_{t-}, M_t) F(dy)dt]$$
$$= E[\int_0^T \lambda \int_{\mathbb{R}} \frac{1}{n!} \sum_{n=1}^{\infty} \frac{\partial^n f}{\partial x^n}(-y)^n F(dy)dt]$$
$$= E[\int_0^T \lambda \frac{1}{n!} \sum_{n=1}^{\infty} \frac{\partial^n f}{\partial x^n} \int_{\mathbb{R}} (-y)^n F(dy)dt]$$
$$= E[\int_0^T \lambda \frac{1}{n!} \sum_{n=1}^{\infty} \frac{\partial^n f}{\partial x^n} E[(-Y)^n]dt].$$

Assuming $\frac{\partial^n f}{\partial x^n}$ is negligible when $n > 2$, then:

(2.9)
$$E[\int_0^T \lambda \int_{\mathbb{R}} f(t, X_{t-} + y, M_t) - f(t, X_{t-}, M_t) F(dy)dt]$$
$$\approxeq E[\int_0^T \lambda \left(-\frac{\partial f}{\partial x}E[Y] + \frac{1}{2}\frac{\partial^2 f}{\partial x^2}E[Y^2]\right) dt].$$

Therefore, (2.7) can be written as:

(2.10)
$$\begin{aligned}&E[f(T,X_T,M_T)]-f(0,X_0,M_0)\\&=E[\int_0^T\left(\frac{\partial f}{\partial t}+\frac{\partial f}{\partial x}(b-\lambda E[Y])+\frac{\partial f}{\partial m}b_1+\frac{1}{2}\frac{\partial^2 f}{\partial x^2}(\sigma^2+\lambda E[Y^2])+\frac{1}{2}\frac{\partial^2 f}{\partial m^2}\sigma_1^2\right)dt]\\&=\int_{\mathbb{R}}\int_{\mathbb{R}}\left[\int_0^T\left(\frac{\partial f}{\partial t}+\frac{\partial f}{\partial x}(b-\lambda E[Y])+\frac{\partial f}{\partial m}b_1+\frac{1}{2}\frac{\partial^2 f}{\partial x^2}(\sigma^2+\lambda E[Y^2])+\frac{1}{2}\frac{\partial^2 f}{\partial m^2}\sigma_1^2\right)\right]\\&\qquad P(t,x,m|0,X_0,M_0)dtdxdm.\end{aligned}$$

Evaluate the right side term by term, then for the first term:

$$\begin{aligned}\int_{\mathbb{R}}\int_{\mathbb{R}}\int_0^T\frac{\partial f}{\partial t}Pdtdxdm&=\int_{\mathbb{R}}\int_{\mathbb{R}}[f\cdot P|_0^T-\int_0^T\frac{\partial P}{\partial t}fdt]dxdm\\&=-\int_{\mathbb{R}}\int_{\mathbb{R}}\int_0^T\frac{\partial P}{\partial t}fdtdxdm.\end{aligned}\tag{2.11}$$

For simplicity, we write $f(t,X_t,M_t),P(t,x,m|0,X_0,M_0)$ as f and P.

The second term:

$$\begin{aligned}&\int_{\mathbb{R}}\int_{\mathbb{R}}\int_0^T\frac{\partial f}{\partial x}(b-\lambda E[Y])Pdtdxdm\\&=\int_{\mathbb{R}}\int_0^T\int_{\mathbb{R}}\frac{\partial f}{\partial x}(b-\lambda E[Y])Pdxdtdm\\&=\int_{\mathbb{R}}\int_0^T\left[f\cdot(b-\lambda E[Y])\cdot P|_{\mathbb{R}}-\int_{\mathbb{R}}\frac{\partial(Pb)}{\partial x}fdx+\int_{\mathbb{R}}\frac{\partial P}{\partial x}\lambda E[Y]fdx\right]dtdm\\&=-\int_{\mathbb{R}}\int_{\mathbb{R}}\int_0^T(\frac{\partial(Pb)}{\partial x}-\lambda E[Y]\frac{\partial P}{\partial x})fdtdxdm.\end{aligned}\tag{2.12}$$

The third term:

$$\begin{aligned}\int_{\mathbb{R}}\int_{\mathbb{R}}\int_0^T\frac{\partial f}{\partial m}b_1Pdtdxdm&=\int_{\mathbb{R}}\int_0^T\int_{\mathbb{R}}\frac{\partial f}{\partial m}b_1Pdmdtdx\\&=\int_{\mathbb{R}}\int_0^T\left[f\cdot b_1\cdot P|_{\mathbb{R}}-\int_{\mathbb{R}}\frac{\partial(Pb_1)}{\partial m}fdm\right]dtdx\\&=-\int_{\mathbb{R}}\int_{\mathbb{R}}\int_0^T\frac{\partial(Pb_1)}{\partial m}fdtdxdm.\end{aligned}\tag{2.13}$$

The fourth term:

(2.14)

$$\begin{aligned}
&\int_{\mathbb{R}}\int_{\mathbb{R}}\int_0^T \frac{1}{2}\frac{\partial^2 f}{\partial x^2}(\sigma^2+\lambda E[Y^2])Pdtdxdm \\
&= \int_{\mathbb{R}}\int_0^T\int_{\mathbb{R}} \frac{1}{2}\frac{\partial^2 f}{\partial x^2}(\sigma^2+\lambda E[Y^2])Pdxdtdm \\
&= \frac{1}{2}\int_{\mathbb{R}}\int_0^T \left[\frac{\partial f}{\partial x}\cdot(\sigma^2+\lambda E[Y^2])\cdot P|_{\mathbb{R}} - \int_{\mathbb{R}}\frac{\partial(P\sigma^2)}{\partial x}\frac{\partial f}{\partial x}dx - \int_{\mathbb{R}}\frac{\partial P}{\partial x}\lambda E[Y^2]\frac{\partial f}{\partial x}dx\right]dtdm \\
&= \frac{1}{2}\int_{\mathbb{R}}\int_0^T \left[-f\cdot(\frac{\partial(P\sigma^2)}{\partial x}+\lambda E[Y^2]\frac{\partial P}{\partial x})|_{\mathbb{R}} + \int_{\mathbb{R}}\frac{\partial^2(P\sigma^2)}{\partial x^2}fdx + \int_{\mathbb{R}}\frac{\partial^2 P}{\partial x^2}\lambda E[Y^2]fdx\right]dtdm \\
&= \int_{\mathbb{R}}\int_{\mathbb{R}}\int_0^T \frac{1}{2}(\frac{\partial^2(P\sigma^2)}{\partial x^2}+\lambda E[Y^2]\frac{\partial^2 P}{\partial x^2})fdtdxdm.
\end{aligned}$$

The fifth term:

$$\begin{aligned}
\int_{\mathbb{R}}\int_{\mathbb{R}}\int_0^T \frac{1}{2}\frac{\partial^2 f}{\partial m^2}\sigma_1^2 Pdtdxdm &= \int_{\mathbb{R}}\int_0^T\int_{\mathbb{R}} \frac{1}{2}\frac{\partial^2 f}{\partial m^2}\sigma_1^2 Pdmdtdx \\
&= \frac{1}{2}\int_{\mathbb{R}}\int_0^T\left[\frac{\partial f}{\partial m}\sigma_1^2 P|_{\mathbb{R}} - \int_{\mathbb{R}}\frac{\partial(P\sigma_1^2)}{\partial m}\frac{\partial f}{\partial m}dm\right]dtdx \\
&= \frac{1}{2}\int_{\mathbb{R}}\int_0^T\left[-f\frac{\partial(P\sigma_1^2)}{\partial m}|_{\mathbb{R}} + \int_{\mathbb{R}}\frac{\partial^2(P\sigma_1^2)}{\partial m^2}fdm\right]dtdx \\
&= \int_{\mathbb{R}}\int_{\mathbb{R}}\int_0^T \frac{1}{2}\frac{\partial^2(P\sigma_1^2)}{\partial m^2}fdtdmdx.
\end{aligned} \tag{2.15}$$

In conclusion, we get the following equation:

$$\begin{aligned}
&E[f(t,X_T,M_T)] - f(0,X_0,M_0) = \\
&\int_{\mathbb{R}}\int_{\mathbb{R}}\int_0^T [-\frac{\partial P}{\partial t} - (\frac{\partial(Pb)}{\partial x}+\lambda E[Y]\frac{\partial P}{\partial x}) - \frac{\partial(Pb_1)}{\partial m} \\
&+\frac{1}{2}(\frac{\partial^2(P\sigma^2)}{\partial x^2}+\lambda E[Y^2]\frac{\partial^2 P}{\partial x^2}) + \frac{1}{2}\frac{\partial^2(P\sigma_1^2)}{\partial m^2}]fdtdxdm.
\end{aligned} \tag{2.16}$$

We know $E[f(T,X_T,M_T)]-f(0,X_0,M_0) = 0$ since $f(T,X_T,M_T) = f(0,X_0,M_0) = 0$ which implies

$$\begin{aligned}
&-\frac{\partial P}{\partial t} - (\frac{\partial(Pb)}{\partial x} - \lambda E[Y]\frac{\partial P}{\partial x}) - \frac{\partial(Pb_1)}{\partial m} \\
&+\frac{1}{2}(\frac{\partial^2(P\sigma^2)}{\partial x^2}+\lambda E[Y^2]\frac{\partial^2 P}{\partial x^2}) + \frac{1}{2}\frac{\partial^2(P\sigma_1^2)}{\partial m^2} = 0,
\end{aligned}$$

then

$$\begin{aligned}
\frac{\partial P}{\partial t} &= -(\frac{\partial(Pb)}{\partial x} - \lambda E[Y]\frac{\partial P}{\partial x}) - \frac{\partial(Pb_1)}{\partial m} + \frac{1}{2}(\frac{\partial^2(P\sigma^2)}{\partial x^2} \\
&+\lambda E[Y^2]\frac{\partial^2 P}{\partial x^2}) + \frac{1}{2}\frac{\partial^2(P\sigma_1^2)}{\partial m^2}.
\end{aligned} \tag{2.17}$$

□

By Proposition 8.14 of [7], for the following two diffusion processes:

(2.18)
$$\begin{cases} X_t := X_0 + \int_0^t b(s, X_s, M_s)ds + \int_0^t \sigma(s, X_s, M_S)dB_s + \int_0^t \sigma_1(s, X_s, M_S)dB^1_s - \sum_{i=1}^{N_t} Y_i, \\ M_t := M_0 + \int_0^t b_1(s, X_s, M_s)ds + \int_0^t \sigma_2(s, X_s, M_s)dB^1_s, \end{cases}$$

where $E[B_tB^1_t] = \rho t$, we have

$$\begin{aligned} df = &\big(\frac{\partial f}{\partial t} + \frac{\partial f}{\partial x}b + \frac{\partial f}{\partial m}b_1 + \frac{1}{2}\frac{\partial^2 f}{\partial x^2}(\sigma^2 + \sigma_1^2 + 2\sigma\sigma_1\rho) \\ &+ \frac{\partial^2 f}{\partial x\partial m}(\sigma_1\sigma_2 + \sigma\sigma_2\rho) + \frac{1}{2}\frac{\partial^2 f}{\partial m^2}\sigma_2^2\big)dt \\ &+ \frac{\partial f}{\partial x}\sigma dB_t + \frac{\partial f}{\partial m}\sigma_2 dB^1_t + \left[f(t, X_{t-} - Y, M_t) - f(t, X_{t-}, M_t)\right]. \end{aligned} \tag{2.19}$$

Therefore, with Theorem 2.1, we can easily derive the Fokker-Planck equation for X_t, M_t in (2.18). $P(t, X_t, M_t)$ is the joint distribution denoted by P:

$$\begin{aligned} \frac{\partial P}{\partial t} = &-(\frac{\partial (Pb)}{\partial x} - \lambda E[Y]\frac{\partial P}{\partial x}) - \frac{\partial (Pb_1)}{\partial m} \\ &+ \frac{1}{2}(\frac{\partial^2[P(\sigma^2 + \sigma_1^2 + 2\sigma\sigma_1\rho)]}{\partial x^2} + \lambda E[Y^2]\frac{\partial^2 P}{\partial x^2}) \\ &+ \frac{1}{2}\frac{\partial^2(P\sigma_2^2)}{\partial m^2} + \frac{\partial^2[P(\sigma_1\sigma_2 + \sigma\sigma_2\rho)]}{\partial x\partial m}. \end{aligned} \tag{2.20}$$

3. Numerical Examples

3.1. A Brief of the High-Dimensional Chang-Cooper Scheme.

Suppose we have the following FP equation:

$$\begin{aligned} \partial_t f(\mathbf{x}, t) - \sum_{i,j=1}^{d} \partial^2_{x_i,x_j}(a_{ij}(\mathbf{x}, t)f(\mathbf{x}, t)) + \sum_{i=1}^{d} \partial_{x_i}(b_i(\mathbf{x}, t)f(\mathbf{x}, t)) = 0, \\ f(\mathbf{x}, , 0) = f_0(\mathbf{x}), \end{aligned} \tag{3.1}$$

where $(\mathbf{x}, t) \in \Omega \times (0, T)$, $\Omega \subset \mathbb{R}^d$ and $f_0(\mathbf{x})$ is the chosen initial distribution, and

$$f = f(\mathbf{x}, t),\ \partial_t f = \frac{\partial f(\mathbf{x}, t)}{\partial t},\ \partial_{x_i} f = \frac{\partial f(\mathbf{x}, t)}{\partial x_i},\ \partial^2_{x_i,x_j} f = \frac{\partial^2 f(\mathbf{x}, t)}{\partial x_i \partial x_j}.$$

Define the flux at the i-th direction as

$$F^i(\mathbf{x}, t) = \sum_{j=1}^{d} a_{ij}(\mathbf{x}, t)\partial_{x_j} f(\mathbf{x}, t) + \left[\sum_{j=1}^{d} \partial_{x_j} a_{ij}(\mathbf{x}, t) - b_i(\mathbf{x}, t)\right] f(\mathbf{x}, t), \tag{3.2}$$

and denote $C^{ij} = a_{ij}(\mathbf{x}, t)$, $B^i = \sum_{j=1}^{d} \partial_{x_j} a_{ij}(\mathbf{x}, t) - b_i(\mathbf{x}, t)$, then (3.2) can be written as

$$F^i(\mathbf{x}, t) = \sum_{j=1}^{d} C^{ij}\partial_{x_j} f + B^i f, \tag{3.3}$$

and we assume that C^{ij} is a positive continuous scalar function for all i, j and B^i satisfies the Lipschitz continuity for all i.

Suppose the time-step size is defined by $\Delta t = \frac{T}{T_{\text{upper}}}$ where T_{upper} is a positive number, then $n\Delta t,\ n = 0, 1, \cdots, T_{\text{upper}}$ are the time steps. Considering $\Omega = (0, L)^d$, an uniform mesh size is applied: $h = \frac{L}{L_{\text{upper}}}$ where L_{upper} is another positive number. The following system is used to represent the spatial position

$$\Omega_h = \{\mathbf{x_m} \in \mathbb{R}^d : \mathbf{x_m} = \mathbf{m}h, \mathbf{m} \in \mathbb{Z}^d\} \cap \Omega.$$

We denote the unit vector by $\mathbf{1}_i$:

$$\mathbf{1}_i = (0, \cdots, 0, 1, 0, \cdots, 0)^T,\ i = 1, 2, \cdots, d,$$

where 1 is the i-th element in the vector.

We consider the following backward first-order time-difference scheme:

$$\frac{\partial f(\mathbf{x_m}, n\Delta t)}{\partial t} = \frac{1}{\Delta t}(f^{n+1}_{\mathbf{m}} - f^n_{\mathbf{m}}), \tag{3.4}$$

where $f^n_{\mathbf{m}} = f(\mathbf{x_m}, n\Delta t)$. Denote $\frac{\partial f(\mathbf{x_m}, n\Delta t)}{\partial t}$ by $\partial_t f^n_{\mathbf{m}}$ for simplicity.

Moreover, with the zero-flux boundary condition $F_{-\frac{1}{2}} = F_{L_{\text{upper}}+\frac{1}{2}} = 0$, the following discretization scheme is applied:

$$\partial_t f^n_{\mathbf{m}} = \frac{1}{h}\sum_{i=1}^{d}(F^{i,n}_{\mathbf{m}+\frac{1}{2}\cdot\mathbf{1}_i} - F^{i,n}_{\mathbf{m}-\frac{1}{2}\cdot\mathbf{1}_i}), \tag{3.5}$$

and the details of $F^{i,n}_{\mathbf{m}+\frac{1}{2}\cdot\mathbf{1}_i}$ and $F^{i,n}_{\mathbf{m}-\frac{1}{2}\cdot\mathbf{1}_i}$ are given later.

Combining (3.4) and (3.5), the full picture of our scheme is as follows:

$$\frac{f^{n+1}_{\mathbf{m}} - f^n_{\mathbf{m}}}{\Delta t} = \frac{1}{h}\sum_{i=1}^{d}(F^{i,n}_{\mathbf{m}+\frac{1}{2}\cdot\mathbf{1}_i} - F^{i,n}_{\mathbf{m}-\frac{1}{2}\cdot\mathbf{1}_i}). \tag{3.6}$$

By [6], we want to find the $\delta^{i,n}_{\mathbf{m}} \in [0, \frac{1}{2}]$ for

$$f^n_{\mathbf{m}+\frac{1}{2}\cdot\mathbf{1}_i} = (1 - \delta^{i,n}_{\mathbf{m}})f^n_{\mathbf{m}+\mathbf{1}_i} + \delta^{i,n}_{\mathbf{m}} f^n_{\mathbf{m}}, \tag{3.7}$$

which is capable to guarantee the positivity of the scheme. Here, $f^n_{\mathbf{m}+\mathbf{1}_i} = f(\mathbf{x_m} + h\mathbf{1}_i, n\Delta t)$.

Therefore, from the definition (3.2), we have

$$F^{i,n}_{\mathbf{m}+\frac{1}{2}\cdot\mathbf{1}_i} = \sum_{j=1}^{d}(C^{ij,n}\partial_{x_j} f^n)_{\mathbf{m}+\frac{1}{2}\cdot\mathbf{1}_i} + (B^{i,n}f^n)_{\mathbf{m}+\frac{1}{2}\cdot\mathbf{1}_i}, \tag{3.8}$$

where

$$B^{i,n}_{\mathbf{m}+\frac{1}{2}\cdot\mathbf{1}_i} = \frac{1}{2}(B^{i,n}_{\mathbf{m}} + B^{i,n}_{\mathbf{m}+\mathbf{1}_i}),\ B^{i,n}_{\mathbf{m}} = B^i(\mathbf{x}_m, n\Delta t) \text{ and } B^{i,n}_{\mathbf{m}+\mathbf{1}_i} = B^i(\mathbf{x}_m + h\mathbf{1}_i, n\Delta t),$$

and

$$C^{ij,n}_{\mathbf{m}+\frac{1}{2}\cdot\mathbf{1}_i} = \frac{1}{2}(C^{ij,n}_{\mathbf{m}} + C^{ij,n}_{\mathbf{m}+\mathbf{1}_i}),\ C^{ij,n}_{\mathbf{m}} = C^{ij}(\mathbf{x}_m, n\Delta t) \text{ and } C^{ij,n}_{\mathbf{m}+\mathbf{1}_i} = C^{ij}(\mathbf{x}_m + h\mathbf{1}_i, n\Delta t).$$

From (3.7), we have

$$\partial_{x_j} f^n_{\mathbf{m}+\frac{1}{2}\cdot\mathbf{1}_i} = (1-\delta^{i,n}_{\mathbf{m}})\partial_{x_j} f^n_{\mathbf{m}+\mathbf{1}_i} + \delta^{i,n}_{\mathbf{m}}\partial_{x_j} f^n_{\mathbf{m}}. \tag{3.9}$$

We approximate $\partial_{x_j} f^n_{\mathbf{m}+\mathbf{1}_i}$ and $\partial_{x_j} f^n_{\mathbf{m}}$:

$$\partial_{x_j} f^n_{\mathbf{m}+\mathbf{1}_i} \approxeq \frac{1}{h}(f^n_{\mathbf{m}+\mathbf{1}_i+\mathbf{1}_j} - f^n_{\mathbf{m}+\mathbf{1}_i}), \tag{3.10}$$

and

$$\partial_{x_j} f^n_{\mathbf{m}} \approxeq \frac{1}{h}(f^n_{\mathbf{m}+\mathbf{1}_j} - f^n_{\mathbf{m}}). \tag{3.11}$$

Plugging (3.9), (3.10) and (3.11) back into (3.8), we have

$$\begin{aligned}
F^{i,n}_{\mathbf{m}+\frac{1}{2}\cdot\mathbf{1}_i} &= \sum_{j=1}^{d}\left[C^{ij,n}_{\mathbf{m}+\frac{1}{2}\cdot\mathbf{1}_i}[\frac{(1-\delta^{i,n}_{\mathbf{m}})}{h}(f^n_{\mathbf{m}+\mathbf{1}_i+\mathbf{1}_j} - f^n_{\mathbf{m}+\mathbf{1}_i}) + \frac{\delta^{i,n}_{\mathbf{m}}}{h}(f^n_{\mathbf{m}+\mathbf{1}_j} - f^n_{\mathbf{m}})]\right] \\
&\quad + B^{i,n}_{\mathbf{m}+\frac{1}{2}\cdot\mathbf{1}_i}[(1-\delta^{i,n}_{\mathbf{m}})f^n_{\mathbf{m}+\mathbf{1}_i} + \delta^{i,n}_{\mathbf{m}} f^n_{\mathbf{m}}] \\
&= \frac{(1-\delta^{i,n}_{\mathbf{m}})}{h}\sum_{j=1}^{d}(C^{ij,n}_{\mathbf{m}+\frac{1}{2}\cdot\mathbf{1}_i} f^n_{\mathbf{m}+\mathbf{1}_i+\mathbf{1}_j}) \\
&\quad + (1-\delta^{i,n}_{\mathbf{m}})(B^{i,n}_{\mathbf{m}+\frac{1}{2}\cdot\mathbf{1}_i} - \frac{1}{h}\sum_{j=1}^{d} C^{ij,n}_{\mathbf{m}+\frac{1}{2}\cdot\mathbf{1}_i}) f^n_{\mathbf{m}+\mathbf{1}_i} \\
&\quad + \frac{\delta^{i,n}_{\mathbf{m}}}{h}\sum_{j=1}^{d}(C^{ij,n}_{\mathbf{m}+\frac{1}{2}\cdot\mathbf{1}_i} f^n_{\mathbf{m}+\mathbf{1}_j}) + \delta^{i,n}_{\mathbf{m}}(B^{i,n}_{\mathbf{m}+\frac{1}{2}\cdot\mathbf{1}_i} - \frac{1}{h}\sum_{j=1}^{d} C^{ij,n}_{\mathbf{m}+\frac{1}{2}\cdot\mathbf{1}_i}) f^n_{\mathbf{m}}.
\end{aligned} \tag{3.12}$$

With the similar notations, we have:

$$\begin{aligned}
F^{i,n}_{\mathbf{m}-\frac{1}{2}\cdot\mathbf{1}_i} &= \frac{(1-\delta^{i,n}_{\mathbf{m}})}{h}\sum_{j=1}^{d}(C^{ij,n}_{\mathbf{m}-\frac{1}{2}\cdot\mathbf{1}_i} f^n_{\mathbf{m}-\mathbf{1}_i+\mathbf{1}_j}) \\
&\quad + (1-\delta^{i,n}_{\mathbf{m}})(B^{i,n}_{\mathbf{m}-\frac{1}{2}\cdot\mathbf{1}_i} - \frac{1}{h}\sum_{j=1}^{d} C^{ij,n}_{\mathbf{m}-\frac{1}{2}\cdot\mathbf{1}_i}) f^n_{\mathbf{m}-\mathbf{1}_i} \\
&\quad + \frac{\delta^{i,n}_{\mathbf{m}}}{h}\sum_{j=1}^{d}(C^{ij,n}_{\mathbf{m}-\frac{1}{2}\cdot\mathbf{1}_i} f^n_{\mathbf{m}+\mathbf{1}_j}) \\
&\quad + \delta^{i,n}_{\mathbf{m}}(B^{i,n}_{\mathbf{m}-\frac{1}{2}\cdot\mathbf{1}_i} - \frac{1}{h}\sum_{j=1}^{d} C^{ij,n}_{\mathbf{m}-\frac{1}{2}\cdot\mathbf{1}_i}) f^n_{\mathbf{m}}.
\end{aligned} \tag{3.13}$$

By $\partial_t f = \nabla \cdot F$ and (3.3), following [6], we want to find the equilibrium solution $\partial_t f = 0 \Leftrightarrow F = 0$. Considering $F^{i,n}_{\mathbf{m}+\frac{1}{2}\cdot\mathbf{1}_i} = 0$, then (3.12) is equivalent to

$$\begin{aligned}&\left[\frac{(1-\delta^{i,n}_{\mathbf{m}})}{h}\sum_{j=1}^{d}(C^{ij,n}_{\mathbf{m}+\frac{1}{2}\cdot\mathbf{1}_i}\frac{f^n_{\mathbf{m}+\mathbf{1}_i+\mathbf{1}_j}}{f^n_{\mathbf{m}+\mathbf{1}_i}})\right.\\ &\left.+(1-\delta^{i,n}_{\mathbf{m}})(B^{i,n}_{\mathbf{m}+\frac{1}{2}\cdot\mathbf{1}_i}-\frac{1}{h}\sum_{j=1}^{d}C^{ij,n}_{\mathbf{m}+\frac{1}{2}\cdot\mathbf{1}_i})\right]\frac{f^n_{\mathbf{m}+\mathbf{1}_i}}{f^n_{\mathbf{m}}}\\ &+\frac{\delta^{i,n}_{\mathbf{m}}}{h}\sum_{j=1}^{d}(C^{ij,n}_{\mathbf{m}+\frac{1}{2}\cdot\mathbf{1}_i}\frac{f^n_{\mathbf{m}+\mathbf{1}_j}}{f^n_{\mathbf{m}}})+\delta^{i,n}_{\mathbf{m}}(B^{i,n}_{\mathbf{m}+\frac{1}{2}\cdot\mathbf{1}_i}-\frac{1}{h}\sum_{j=1}^{d}C^{ij,n}_{\mathbf{m}+\frac{1}{2}\cdot\mathbf{1}_i})=0.\end{aligned} \tag{3.14}$$

[2] and [17] applied the following approximation by assuming that the stochastic process has a diagonal diffusion matrix:

$$\frac{f^n_{\mathbf{m}+\mathbf{1}_i}}{f^n_{\mathbf{m}}} = exp(-\frac{B^{i,n}_{\mathbf{m}+\frac{1}{2}\cdot\mathbf{1}_i}}{C^{ii,n}_{\mathbf{m}+\frac{1}{2}\cdot\mathbf{1}_i}}h).$$

In [9], the same approximation was used. However, with a different reasoning: following the Goodman's prescription, the cross terms are neglected because the strongest variation fo the distribution function is in the energy direction when modeling the dynamical evolution of star clusters with the FPE. [21] developed a similar but not identical method. In our case, the following approximation is used to account for the impacts of the cross terms:

$$\frac{f^n_{\mathbf{m}+\mathbf{1}_i}}{f^n_{\mathbf{m}}} = exp(-\frac{1}{d}\sum_{j=1}^{d}\frac{B^{i,n}_{\mathbf{m}+\frac{1}{2}\cdot\mathbf{1}_i}}{C^{ij,n}_{\mathbf{m}+\frac{1}{2}\cdot\mathbf{1}_i}}h). \tag{3.15}$$

Moreover, consider

$$F^{i,n}_{\mathbf{m}+\mathbf{1}_i} = \sum_{j=1}^{d}(C^{ij,n}\partial_{x_j}f^n)_{\mathbf{m}+\mathbf{1}_i} + (B^{i,n}f^n)_{\mathbf{m}+\mathbf{1}_i} = 0,$$

which implies

$$\partial_{x_j}f^n_{\mathbf{m}+\mathbf{1}_i} = -\frac{B^{i,n}_{\mathbf{m}+\mathbf{1}_i}/d}{C^{ij,n}_{\mathbf{m}+\mathbf{1}_i}}f^n_{\mathbf{m}+\mathbf{1}_i}. \tag{3.16}$$

Using the same approximation for the partial derivatives as above, we get

$$\frac{f_{\mathbf{m}+\mathbf{1}_i+\mathbf{1}_j}-f_{\mathbf{m}+\mathbf{1}_i}}{h} = -\frac{B^{i,n}_{\mathbf{m}+\mathbf{1}_i}/d}{C^{ij,n}_{\mathbf{m}+\mathbf{1}_i}}f_{\mathbf{m}+\mathbf{1}_i},$$

which gives us

$$\frac{f_{\mathbf{m}+\mathbf{1}_i+\mathbf{1}_j}}{f_{\mathbf{m}+\mathbf{1}_i}} = -\frac{h}{d}\frac{B^{i,n}_{\mathbf{m}+\mathbf{1}_i}}{C^{ij,n}_{\mathbf{m}+\mathbf{1}_i}}+1. \tag{3.17}$$

Combining (3.14), (3.15), and (3.17) yields $\delta^{i,n}_{\mathbf{m}}$.

In our case, $d=2$, therefore, by (3.14), (3.15) and (3.17), we have:

$$\tilde{A}(1-\delta^{i,n}_{\mathbf{m}})+\tilde{B}\delta^{i,n}_{\mathbf{m}}+\tilde{C}\delta^{i,n}_{\mathbf{m}}=0 \implies \delta^{i,n}_{\mathbf{m}}=\frac{\tilde{A}}{\tilde{A}-\tilde{B}-\tilde{C}}, \tag{3.18}$$

where

$$\begin{aligned} \tilde{A} &= [B^{i,n}_{\mathbf{m}+\frac{1}{2}\cdot\mathbf{1}_i}-\frac{B^{i,n}_{\mathbf{m}+\mathbf{1}_i}}{4}(2+\frac{C^{i1,n}_{\mathbf{m}}}{C^{i1,n}_{\mathbf{m}+\mathbf{1}_i}}+\frac{C^{i2,n}_{\mathbf{m}}}{C^{i2,n}_{\mathbf{m}+\mathbf{1}_i}})]\tilde{D},\\ \tilde{B} &= \frac{1}{h}\left[C^{i1,n}_{\mathbf{m}+\frac{1}{2}\cdot\mathbf{1}_i}exp(-\frac{h}{2}\sum_{j=1}^{2}\frac{B^{1,n}_{\mathbf{m}+\frac{1}{2}\cdot\mathbf{1}_1}}{C^{1j,n}_{\mathbf{m}+\frac{1}{2}\cdot\mathbf{1}_1}})+C^{i2,n}_{\mathbf{m}+\frac{1}{2}\cdot\mathbf{1}_i}exp(-\frac{h}{2}\sum_{j=1}^{2}\frac{B^{2,n}_{\mathbf{m}+\frac{1}{2}\cdot\mathbf{1}_2}}{C^{2j,n}_{\mathbf{m}+\frac{1}{2}\cdot\mathbf{1}_2}})\right],\\ \tilde{C} &= B^{i,n}_{\mathbf{m}+\frac{1}{2}\cdot\mathbf{1}_i}-\frac{1}{h}\sum_{j=1}^{2}C^{ij,n}_{\mathbf{m}+\frac{1}{2}\cdot\mathbf{1}_i},\\ \tilde{D} &= exp(-\frac{h}{2}\sum_{j=1}^{2}\frac{B^{i,n}_{\mathbf{m}+\frac{1}{2}\cdot\mathbf{1}_i}}{C^{ij,n}_{\mathbf{m}+\frac{1}{2}\cdot\mathbf{1}_i}}). \end{aligned} \tag{3.19}$$

For the diagonal diffusion matrix case, such as in [2] and [17], they have

$$\delta^{i,n}_{\mathbf{m}}=\frac{C^{ii,n}_{\mathbf{m}+\frac{1}{2}\cdot\mathbf{1}_i}}{hB^{i,n}_{\mathbf{m}+\frac{1}{2}\cdot\mathbf{1}_i}}-\frac{1}{exp[(hB^{i,n}_{\mathbf{m}+\frac{1}{2}\cdot\mathbf{1}_i})/(C^{ii,n}_{\mathbf{m}+\frac{1}{2}\cdot\mathbf{1}_i})]-1},$$

which is quite different from us.

Above is the sketch of the high-dimensional Chang-Cooper scheme for diffusion processes with a non-diagonal covariance matrix. Refer to [6], [15], [2] and [17] for more discussions on the stability, convergence and truncation error for the case with a diagonal diffusion matrix.

3.2. **The Validation of Accuracy.** To illustrate the accuracy of the previous algorithm, we consider the following stochastic process:

$$dX_t = dW_t : X_t = (x_t, y_t)^T. \tag{3.20}$$

It is easy to derive the FPE for X_t:

$$\frac{\partial P(x,y,t)}{\partial t}=\frac{1}{2}\frac{\partial^2 P(x,y,t)}{\partial x^2}+\frac{1}{2}\frac{\partial^2 P(x,y,t)}{\partial y^2}. \tag{3.21}$$

For the multidimensional heat equation:

$$\begin{cases} u_t = k\Delta u, \quad \mathbf{x}\in\mathbb{R}^n, t>0,\\ u(\mathbf{x},0)=\phi(\mathbf{x}). \end{cases} \tag{3.22}$$

The solution is

$$u(\mathbf{x},t)=\int_{\mathbb{R}^n}\phi(Y)u(X-Y)dY, \tag{3.23}$$

which is a convolution operation.

Suppose the initial distribution is $P(x,y,0) = \frac{1}{2\pi}exp(-\frac{x^2+y^2}{2})$, then the solution for (3.21) can be seen as the convolution between the following two random variables:

$$X_1 \sim N(\mu_1, \Sigma_1): \qquad \mu_1 = [0,0], \qquad \Sigma_1 = \begin{bmatrix} 1 & 0 \\ 0 & 1 \end{bmatrix}, \tag{3.24}$$

$$X_2 \sim N(\mu_2, \Sigma_2): \qquad \mu_1 = [0,0], \qquad \Sigma_1 = \begin{bmatrix} t & 0 \\ 0 & t \end{bmatrix}. \tag{3.25}$$

Both random variables follow the bivariate normal distribution, then the convolution between the two is:

$$X \sim N(\mu, \Sigma): \qquad \mu := \mu_1 + \mu_2 = [0,0], \qquad \Sigma = \Sigma_1 + \Sigma_2 = \begin{bmatrix} 1+t & 0 \\ 0 & 1+t \end{bmatrix}. \tag{3.26}$$

Therefore, the analytic solution to (3.21) with the initial distribution $P(x,y,0) = \frac{1}{2\pi}exp(-\frac{x^2+y^2}{2})$ is:

$$P(x,y,t) = \frac{1}{2\pi(1+t)}exp(-\frac{x^2+y^2}{2(1+t)}). \tag{3.27}$$

Applying our scheme for numerical approximation and comparing it with the analytic solution yields Figure 1.

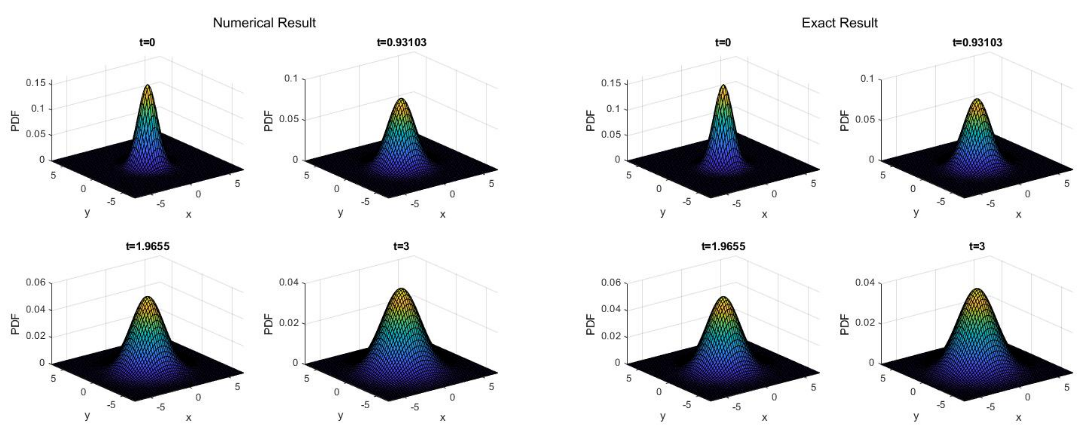

FIGURE 1. The PDFs at different time points of the numerical and exact results

The top subfigure of Figure 1 is the Chang-Cooper scheme numerical approximation for (3.21), and the bottom one is the exact results from (3.27). The distributions at four different time points $t = 0, t = 0.93103, t = 1.9655, t = 3$ are plotted.

In addition to Figure 1, we validate the accuracy of our scheme with the Norm of Error (NOE). The NOE is defined as

$$||e|| = \sqrt{\frac{1}{N}(\sum(P^{\text{num}}_{i,j} - P^{\text{exact}}_{i,j})^2)}. \tag{3.28}$$

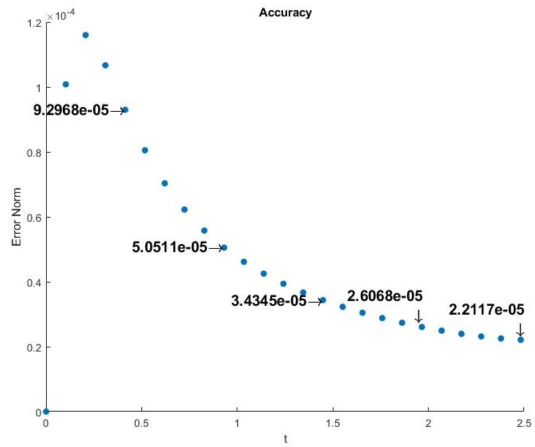

FIGURE 2. The norm of error

Based on Figure 2, the NOE stays at a low level, and it keeps decreasing with time-evolving, which indicate the scheme works well.

3.3. **Impacts of Risk Aversion in the Game.** Combining contents discussed above, we have:

$$\begin{aligned}
B_1 &= b - \lambda E[Y],\\
B_2 &= b_1,\\
C_{11} &= \frac{1}{2}(\sigma_2 + \sigma_1^2 + 2\sigma\sigma_1 + \lambda E[Y^2]),\\
C_{12} = C_{21} &= \frac{1}{2}(\sigma_1\sigma_2 + \sigma\sigma_2\rho),\\
C_{22} &= \frac{1}{2}\sigma_2^2.
\end{aligned}$$

Hence, based on (2.1), for the insurance company A we have:

$$\begin{aligned}
B_1 &= r(X_t - (u_t^1)^2) + (\mu_1 - r)A_t^1 + (c_1 - \delta(q_1))(p_1 u_t^1 + \eta)H\\
&\quad - (c_1 - \delta(q_1))(p_1 u_t^1 + p_2 u_t^2 + 2\eta)M_t - \lambda E[Z^1],\\
B_2 &= (p_1 u_t^1 + \eta)H - (p_1 u_t^1 + p_2 u_t^2 + 2\eta)M_t,\\
C_{11} &= \frac{1}{2}\{(A_t^1\sigma_1)^2 + [(c_1 - \delta(q_1))\sigma_m]^2 + 2A_t^1\sigma_1(c_1 - \delta(q_1))\sigma_m + \lambda E[(Z^1)^2]\},\\
C_{12} = C_{21} &= \frac{1}{2}[A_t^1\sigma_1\sigma_m\rho_1 + (c_1 - \delta(q_1))\sigma_m^2],\\
C_{22} &= \frac{1}{2}\sigma_m^2.
\end{aligned} \tag{3.29}$$

For the insurance company B, we have:

$$(3.30)\quad \begin{aligned} B_1 &= r(Y_t - (u_t^2)^2) + (\mu_2 - r)A_t^2 + (c_2 - \delta(q_2))(p_1 u_t^1 + \eta)H \\ &\quad - (c_2 - \delta(q_2))(p_1 u_t^1 + p_2 u_t^2 + 2\eta)M_t - \lambda E[Z^2], \\ B_2 &= (p_1 u_t^1 + \eta)H - (p_1 u_t^1 + p_2 u_t^2 + 2\eta)M_t, \\ C_{11} &= \frac{1}{2}\{(A_t^2\sigma_2)^2 + [(c_2 - \delta(q_2))\sigma_m]^2 + 2A_t^2\sigma_2(c_2 - \delta(q_2))\sigma_m + \lambda E[(Z^2)^2]\}, \\ C_{12} &= C_{21} = \frac{1}{2}[A_t^2\sigma_2\sigma_m\rho_2 + (c_2 - \delta(q_2))\sigma_m^2], \\ C_{22} &= \frac{1}{2}\sigma_m^2. \end{aligned}$$

In [16], the exponential utility function $J(x) = \gamma - \frac{a}{b}e^{-bx}$ is applied. In the utility function, γ is a desired level determined by experts whom insurance companies hire; a is a coefficient controlling the shape; b is the risk aversion coefficient of insurance companies. Then, the two-control-variables optimal strategies for (2.1) are:

$$(A_1^*, u_1^*) = \left(\frac{(\mu_1 - r) - \rho_1\sigma_1\sigma_m\Delta_1 b}{\sigma_1^2 b e^{r(T-t)}}, \frac{p_1(H - m)\Delta_1}{2re^{r(T-t)}}\right), \tag{3.31}$$

and

$$(A_2^*, u_2^*) = \left(\frac{(\mu_2 - r) + \rho_2\sigma_2\sigma_m\Delta_2 b}{\sigma_2^2 b e^{r(T-t)}}, \frac{p_2 m\Delta_2}{2re^{r(T-t)}}\right), \tag{3.32}$$

where $\Delta_1 = c_1 - \delta(q_1) > 0$ and $\Delta_2 = c_2 - \delta(q_2) > 0$.

To study the relationship between b and the expected utility of terminal wealth $E[J(X_T)]$ the following procedure is developed:

1. Generate wealth paths for X_t, Y_t, M_t and record the states of $X_t, Y_t, u_t^1, u_t^2, A_t^1, A_t^2, m_t$ at each time point;
2. Plug the values getting from Step 1 into (3.29) and (3.30) to approximate the joint distribution $P(x, m, T)$;
3. Run steps 1 and 2 N times and take average of $P(x, m, T)$, the averaged $P(x, m, T)$ is the desired result;
4. Calculate the marginal distribution $P_X(x, T)$ based on the averaged joint PDF, then estimate the parameters for the marginal PDF;
5. Calculate the expectation for the terminal utility function: $E[J(X_T)] = \gamma - \frac{a}{b}E[e^{-bX_T}]$ with the distribution parameters getting from the previous step.

In our case, the previous procedure is modified a little due to the time-saving consideration:

1. Generate N wealth paths for X_t, Y_t, M_t and take the mean for $X_t, Y_t, u_t^1, u_t^2, A_t^1, A_t^2, m_t$ at each time point;
2. Plug the means getting from Step 1 into (3.29) and (3.30) to approximate the joint distribution $P(x, m, T)$;

3. Calculate the marginal distribution $P_X(x,T)$ based on $P(x,m,T)$, then estimate the parameters for the marginal PDF;
4. Calculate the expectation for the terminal utility function: $E[J(X_T)] = \gamma - \frac{a}{b}E[e^{-bX_T}]$ with the distribution parameters getting from the previous step.

The following parameter values are used to generate numerical examples:

TABLE 1. Values of parameters

r	0.02	μ_1	0.04	μ_2	0.06	η	0.01	σ_1	0.08	σ_2	0.13
H	2.00	Δ_1	0.15	Δ_2	0.20	σ_M	0.05	p_1	0.05	p_2	0.04
a	1	q_1	0.6	q_2	0.6	γ	1	λ_1	1.0	λ_2	2.0
Z^1	exp(12)	Z^2	exp(16)	ρ_1	0.10	ρ_2	0.05				

In our case, it is assumed that we have the following initial distribution function:

$$P(x,m,0) = \frac{1}{2\pi\sqrt{Var(X_T)Var(M_T)}}\exp\left(-\frac{(x-\bar{X}_T)^2}{2Var(X_T)} - \frac{(y-\bar{M}_T)^2}{2Var(M_T)}\right), \quad (3.33)$$

which is a bivariate normal distribution which has no interactions between variables at time 0. Besides, we assume that $x \in [\bar{X}_T - 6\sqrt{Var(\bar{X}_T)}, \bar{X}_T + 3\sqrt{Var(\bar{X}_T)}], m \in [\bar{M}_T - 5\sqrt{Var(\bar{M}_T)}, \bar{M}_T + 5\sqrt{Var(\bar{M}_T)}]$. Moreover, due to the similarity between the insurance company A and B, the analysis for company B is skipped here.

To get an accurate approximation of $E[J(X_T)]$, first, we need to figure out the best mesh size. The marginal distributions for X_T and M_T are plotted under various grid settings to observe the difference.

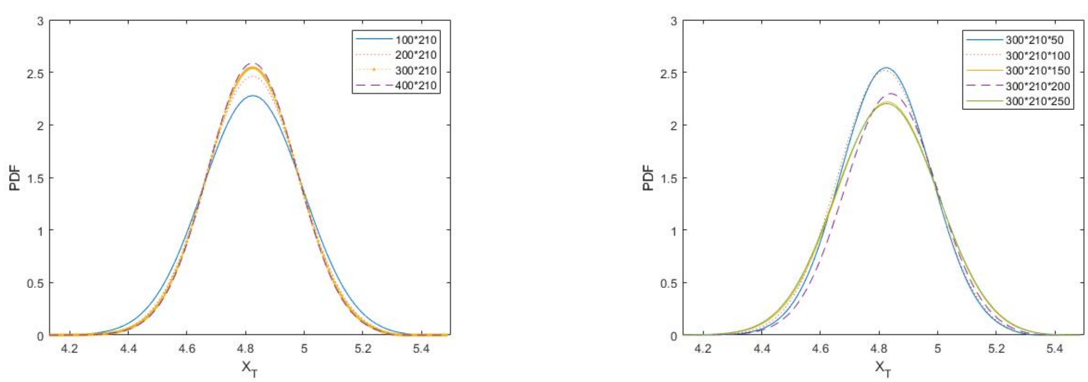

FIGURE 3. The marginal distribution of X_t with different grid settings

The legends of Figure 3 and Figure 4 indicate the number of steps (NOS) for X_t, M_t, t, which is the size of the mesh. The default NOS of t is 50. In this test, the risk aversion coefficient $b = 2$.

From Figure 3 and Figure 4, we can see that the marginal distribution of X_T is more unstable than M_T. In the real case, due to the time consideration, we have

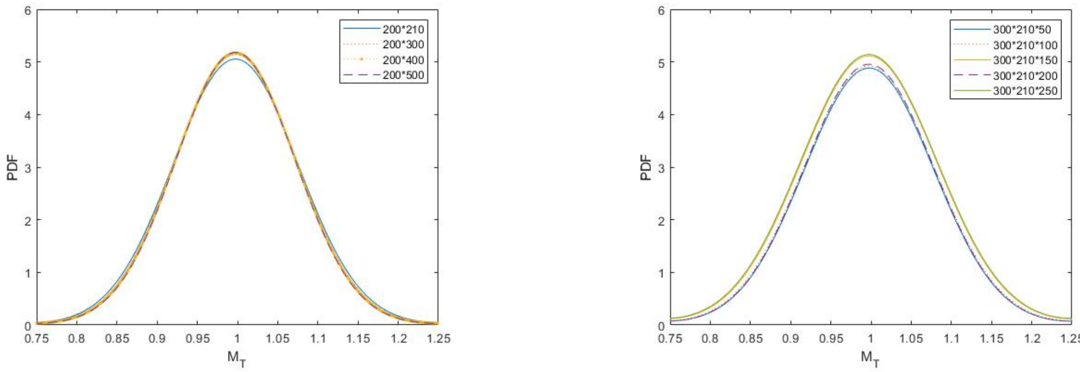

FIGURE 4. The marginal distribution of M_t with different grid settings

to make a trade-off between accuracy and efficiency. Eventually, we believe that the best balance is acquired when the size of the mesh is $300 * 300 * 150$.

By our scheme, we can record the full evolution of the FPE. Hence, we can visually check the joint PDF $P(x, m, t)$ at different time points in Figure 5:

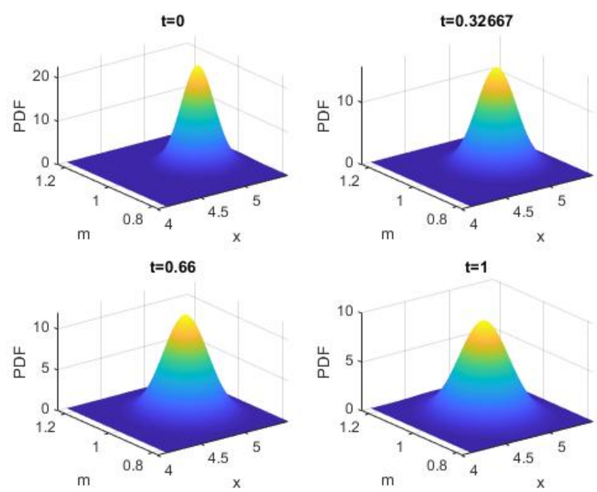

FIGURE 5. The evolution of the joint PDF $P(x, m, t)$

In Figure 5, the joint PDF is more concentrated at the beginning and gets diluted toward the end due to the interaction between X_t and M_t during the evolution. One more thing we can see directly is: starting from a bivariate normal distribution, it seems like the same distribution remains at $T = 1$ by eyes. This claim gets double-checked later with another method.

At last, let us see what impacts the risk aversion coefficient b brings to the expected utility of terminal wealth $E[J(X_T)]$:

Ten different b values with the corresponding $E[J(X_T)]$ are shown in the figure. The larger b value brings larger terminal utility, and the terminal utility is more stable with the growth of b. When b is large enough, based on (3.31), we would have

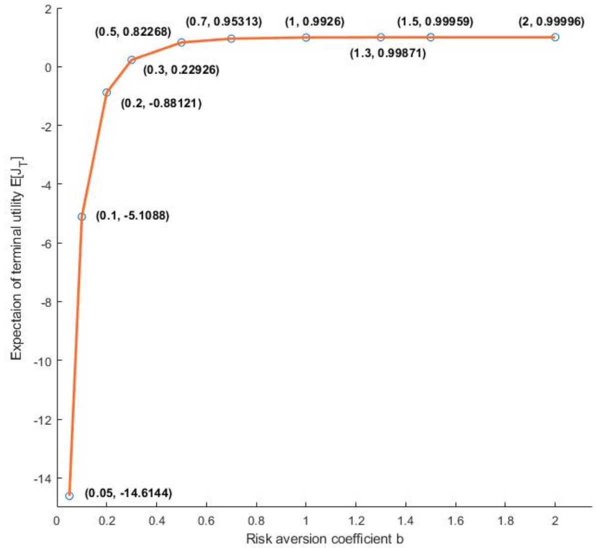

FIGURE 6. The relationship between the risk aversion b and the expected utility of terminal wealth $E[J(X_T)]$

$(A_1^*, u_1^*) \to (0, \frac{p_1(H-m)\Delta_1}{2re^{r(T-t)}})$. We may conclude that due to the stronger risk aversion attitude of player 1, he would choose to allocate more resources on the advertising and leave less money on the investment since the investment directly involving risky assets would be more volatile and risky than the daily business, in our case, which is the periodical collection of insurance premiums and payments of insurance claims. When A_1^* is small enough, the (2.1) is dominated by the market competition and insurance claims, which is a compound Poisson process. Since $\sigma_1 > \sigma_M$, the terminal utility should be more stable when b is large. Moreover, since the exponential utility function is applied in our game, there should be a ceiling for terminal utility due to the nature of the exponential function. The ceiling is around $b = 2$ in the figure. When b gets closer to two, insurance companies approach the pre-set performance target $\gamma = 1$, which agrees with the definition of γ in actuarial science.

We claim that the joint PDF $p(x, m, t)$ at $t = 1$ is still a bivariate normal distribution by a visual check from Figure 5. Here, more evidences are given to support the statement from a statistics perspective. The next table shows how good the fit of the bivariate normal distribution is:

We have a pretty good fit since for all b values, the SSE and RMSE are small, and the adjusted R Square are quite close to 1. The best fit appears in the region around $b = 0.5$. Ten fits have the same DFE (Degree of Freedom in the Error): $90, 596$.

After validating the goodness of our fit, let us see how the parameters evolve for the bivariate normal distribution:

Table 2. The goodness of the bivariate normal distribution fit

b	SSE	R Square	Adj. R Square	RMSE
0.05	31.3931	0.9227	0.9227	0.0186
0.1	152.9850	0.9054	0.9054	0.0411
0.2	164.3679	0.9743	0.9743	0.0426
0.3	90.5360	0.9936	0.9936	0.0316
0.5	0.6706	1.0000	1.0000	0.0027
0.7	1.3890	1.0000	1.0000	0.0039
1.0	2.9999	1.0000	1.0000	0.0058
1.3	5.2888	1.0000	1.0000	0.0076
1.5	7.1824	1.0000	1.0000	0.0089
2.0	13.0339	1.0000	1.0000	0.0120

Table 3. The parameter evolution of the bivariate normal distribution

<table>
<tr><td colspan="4">$t = 0$</td></tr>
<tr><td rowspan="2"></td><td>$\mu_X = 6.2359$</td><td>$\sigma_X = 5.1200$</td><td rowspan="2">$\rho_{X,M} = 0$</td></tr>
<tr><td>$\mu_M = 1.0024$</td><td>$\sigma_M = 0.0459$</td></tr>
<tr><td colspan="4">$t = 1$</td></tr>
<tr><td rowspan="2">$b = 0.05$</td><td>$\mu_X = 4.976$
$[4.899, 5.053]$</td><td>$\sigma_X = 1$
$[0.9907, 1.0090]$</td><td rowspan="2">$\rho_{X,M} = -9.03 \times 10^{-5}$
$[-0.05887, 0.05869]$</td></tr>
<tr><td>$\mu_M = 0$
Fixed at bound</td><td>$\sigma_M = 0.7203$
$[0.7135, 0.7270]$</td></tr>
<tr><td rowspan="2">$b = 1.00$</td><td>$\mu_X = 4.995$
$[4.995, 4.995]$</td><td>$\sigma_X = 0.4209$
$[0.4209, 0.4210]$</td><td rowspan="2">$\rho_{X,M} = -9.03 \times 10^{-5}$
$[-1.057 \times 10^{-4}, -7.485 \times 10^{-6}]$</td></tr>
<tr><td>$\mu_M = 1.001$
$[1.001, 1.001]$</td><td>$\sigma_M = 0.07382$
$[0.07382, 0.07382]$</td></tr>
<tr><td rowspan="2">$b = 2.00$</td><td>$\mu_X = 4.993$
$[4.993, 4.993]$</td><td>$\sigma_X = 0.2524$
$[0.2524, 0.2524]$</td><td rowspan="2">$\rho_{X,M} = -4.432 \times 10^{-5}$
$[-1.057 \times 10^{-4}, 1.707 \times 10^{-5}]$</td></tr>
<tr><td>$\mu_M = 1.001$
$[1.001, 1.001]$</td><td>$\sigma_M = 0.07426$
$[0.07425, 0.07426]$</td></tr>
</table>

In 3, the interval under each parameter is the 95% Confidence Interval (C.I.). We have the same initial distribution for all risk aversions. All C.I.s are pretty narrow, which is another indicator of a good fit. Moreover, we can see that the C.I.s of small b are relatively wider comparing with larger b, which is consistent with 2.

Same as in [20], a Monte-Carlo simulation is carried out for $E[J(X_T)]$ to compare the results between the simulation and numerical method. In the simulation, N paths of X_t, Y_t, M_t under different risk aversions are generated to get X_T, Y_T, M_T. Then we approximate $E[J(X_T)]$ by taking average of $\gamma - \frac{a}{b}e^{-bX_T}$. In the simulation, $N = 5,000$ and the NOS of t is $1,000$. The result is presented in Figure 7.

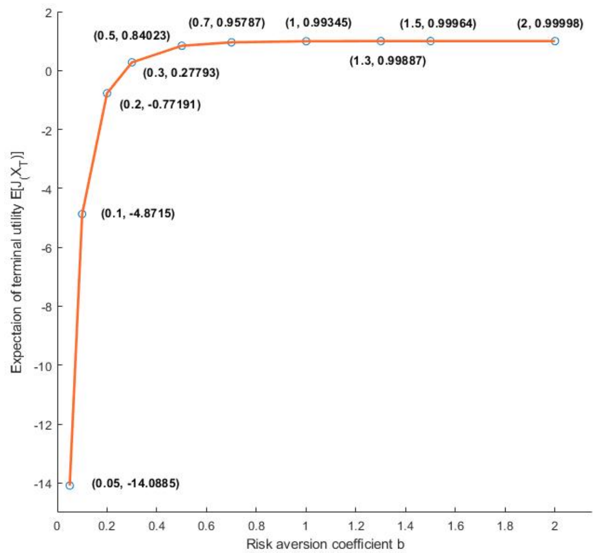

FIGURE 7. The relationship between the risk aversion b and the expected utility of terminal wealth $E[J(X_T)]$ (By the Monte-Carlo simulation)

Figure 7 entirely agrees with Figure 6 except for minor disturbances on numbers. It validates the correctness of our scheme again.

4. **Conclusion**

In this paper, we tried to analyze the role of risk aversion coefficient b in the stochastic reinsurance game. Since PDFs can fully characterize the state of diffusion processes, we derive the associated PDF using the FPE. A more general FPE applicable to high dimensions and with covariance terms is given. The Chang-Cooper scheme is chosen to perform the analysis due to it is easy to understand and implement. Expansions of the scheme are discussed to make it applicable to our problem. A simple example is used to illustrate the accuracy of our scheme. Moreover, a procedure is developed to carry out numerical analysis between the risk aversion b and the expected utility of terminal wealth $E[J(X_T)]$. With the procedure, the exact pattern of the relationship between b and $E[J(X_T)]$ is revealed. In the scenario we gave, a more significant risk aversion coefficient brings more terminal wealth, but the marginal utility of b is subject to the exponential decay. The Monte-Carlo method is also applied to compare the results. The result from the Monte-Carlo method further prove the correctness of our procedure. Further explorations on this research include:

improving the procedure to eliminate the simulation work, incorporating the optimal control derivation into the structure, and adding the multi-player situation.

REFERENCES

[1] M. Annunziato and A. Borzi. Optimal control of probability density functions of stochastic processes. *Mathematical Modeling and Analysis*, 15(4):393 – 407, 2010.

[2] M. Annunziato and A. Borzi. A Fokker-Planck control framework for multidimensional stochastic processes. *Journal of Computational and Applied Mathematics*, 237:487 – 507, 2013.

[3] Taras Bodnar and Yarema Okhrin. Determination and estimation of risk aversion coefficients. *Computational Management Science*, 15:297 – 317, 2018.

[4] Tim Bollerslev, Michael Gibson, and Hao Zhou. Dynamic estimation of volatility risk premia and investor risk aversion from option-implied and realized volatilities. *Journal of Economics*, 160:235 – 245, 2011.

[5] Christophe Buet and Stephane Dellacherie. On the Chang-Cooper scheme applied to a linear Fokker-Planck equation. *Communications in Mathematical Sciences*, 8(4):1079 – 1090, 2010.

[6] J.S. Chang and G. Cooper. A practical difference scheme for Fokker-Planck equations. *Journal of Computational Physics*, 6:1 – 16, 1970.

[7] Rama Cont and Peter Tankov. *Financial Modeling with Jump Processes*. Chapman & Hall/CRC.

[8] James Dow and Sergio Ribeiro Da Costa Werlang. Uncertainty aversion, risk aversion, and the optimal choice of portfolio. *Econometrica*, 60(1):197 – 204, 1992.

[9] G. A. Drukier, H. N. Cohn, P. M. Lugger, and H. Yong. Anisotropic fokker-planck models for the evolution of globular star clusters: The core-halo connection. *The Astrophysical Journal*, 518:233 – 245, 1999.

[10] Arthur Fleig and Roberto Guglielmi. Optimal control of the Fokker-Planck equation with space-dependent controls. *Journal of Optimization Theory of Applications*, 174:408 – 427, 2017.

[11] Charles A. Holt and Susan K. Laury. Risk aversion and incentive effects. *The American Economic Review*, 92(5):1644 – 1655, 2002.

[12] Zhimin Huang and Susan X. Li. Co-op advertising models in manufacturer-retailer supply chains: A game theory approach. *European Journal of Operations Research*, 135:527 – 544, 2001.

[13] Jens Carsten Jackwerth. Recovering risk aversion from option prices and realized returns. *The Review of Financial Studies*, 13(2):433 – 451, 2000.

[14] Miroslav Karny. Towards fully probabilistic control design. *Automatica*, 32(12): 1719 – 1722, 1996.

[15] E. W. Larsen, C. D. Levermore, G. C. Pomraning, and J. G. Sanderson. Discretization methods for one-dimensional Fokker-Planck operators. *Journal of Computational Physics*, 61:359 – 390, 1985.

[16] Negash Medhin and Chuan Xu. Non-zero sum stochastic differential reinsurance game with jump diffusion process. *Journal of Optimization Theory and Applications*, 187:585–606, 2020.

[17] Masoumeh Mohammadi and Alfio Borzi. Analysis of the Chang-Cooper discretization scheme for a class of Fokker-Planck equations. *Journal of Numerical Mathematics*, 0(0):1 – 29, November 2015.

[18] Lorenzo Pareschi and Mattia Zanella. Structure preserving schemes for nonlinear Fokker-Planck equations and applications. *Journal of Scientific Computing*, 74: 1575 – 1600, 2018.

[19] Mir Mehdi SeyedEsfahani, Maryam Biazaran, and Mohsen Gharakhani. A game theoretic approach to coordinate pricing and vertical co-op advertising in manufacturer-retailer supply chains. *European Journal of Operations Research*, 211:263 – 273, 2011.

[20] Paul Sjoberg. Numerical solutions of the Fokker-Planck approximation of the chemical master equation. 2005.

[21] Koji Takahashi. Fokker-planck models of star clusters with anisotropic velocity distributions. i. pre-collapse evolution. *Publications of the Astronomical Society of Japan*, 47:561 – 577, 1995.

[22] P. J. Thomas. Measuring risk-aversion: The challenge. *Measurement*, 79:285 – 301, 2015.

[23] Annette Vissing-Jorgensen and Orazio P. Attanasio. Stock-market participation, intertemporal substitution, and risk-aversion. *The American Economic Review*, 93(2):383 – 391, 2003.